ՀՀ ԳԱԱ Վ. ՀԱՄԲԱՐՁՈՒՄՅԱՆԻ ԱՆՎԱՆ ԲՅՈՒՐԱԿԱՆԻ ԱՍՏՂԱԴԻՏԱՐԱՆ

Իսրայելյան Դավիթ Սամվելի

Բլազարների գերմանուշակագույն և ռենտգենյան հատկությունների ուսումնասիրություն

ՍԵՂՄԱԳԻՐ
Ա.03.02 - «Աստղաֆիզիկա, ռադիոաստղագիտություն»
մասնագիտությամբ ֆիզիկամաթեմատիկական գիտությունների թեկնածուի
գիտական աստիճանի հայցման ատենախոսության

ԵՐԵՎԱՆ-2022

NAS RA BYURAKAN ASTROPHYSICAL OBSERVATORY AFTER V. AMBARTSUMIAN

Israyelyan Davit

Investigation of UV and X-ray properties of blazars

Thesis for the degree of candidate in physical and mathematical sciences
Specialty 01.03.02 – “Astrophysics and Radioastronomy”

SYNOPSIS

YEREVAN-2022

Ատենախոսության թեման հաստատվել է ՀՀ ԳԱԱ Վ. Համբարձումյանի անվան Բյուրականի աստղադիտարանի գիտական խորհրդում:

Գիտական ղեկավար՝

ֆիզ.-մաթ. գիտ. թեկնածու Նարեկ Սահակյան

Պաշտոնական ընդդիմախոսներ՝

1. ֆիզ.-մաթ. գիտ. դոկտոր Գագիկ Տեր-Ղազարյան
2. ֆիզ.-մաթ. գիտ. դոկտոր Գևորգ Հաջյան

Առաջատար կազմակերպություն՝

Երևանի Պետական Համալսարան (ԵՊՀ)

Պաշտպանությունը կայանալու է 2022 թ. դեկտեմբերի 22-ին ժամը 14:00-ին, ՀՀ ԳԱԱ Բյուրականի աստղադիտարանում գործող ՀՀ ԲՈԿ-ի «Աստղագիտություն» 048 մասնագիտական խորհրդի նիստում (0213, Բյուրական, Արագածոտնի մարզ):
Ատենախոսությանը կարելի է ծանոթանալ ՀՀ ԳԱԱ Վ. Համբարձումյանի անվան Բյուրականի աստղադիտարանի գրադարանում:
Սեղմագիրը առաքված է 2022 նոյեմբերի 11-ին:

Մասնագիտական խորհրդի
գիտական քարտուղար՝

ֆիզ.-մաթ. գիտ. թեկնածու
Ելենա Նիկողոսյան

The subject of the dissertation is approved by the scientific council of the NAS RA Byurakan Astrophysical Observatory after V. A. Ambartsumian

Scientific advisor:

Candidate of Phys. Math. Sciences Narek Sahakyan

Official opponents:

1. Doctor of Phys. Math. Sciences Gagik Ter-Kazarian
2. Doctor of Phys. Math. Sciences Gevorg Hajyan

Leading Organization:

Yerevan State University

The defence will take place on 22nd of December 2022 at 14:00 at the meeting of the specialized council of the SCC 048 "Astronomy" of the Byurakan Astrophysical Observatory named after V. Ambartsumian NAS RA (0213, Byurakan, Aragatzotn Prov.).
The dissertation can be found at the Byurakan Astrophysical Observatory library.
The synopsis has been sent out on 11th of November, 2022.

Scientific secretary of
the Special Council

Candidate of Phys. Math. Sciences
Elena Nikighosyan

Relevance and motivation

The observations early in the 20th century already revealed that there are emission lines in the nuclei of some galaxies. Then, due to the progress in radio observations the first quasar was discovered. It initiated intense efforts in studying these new objects, collectively referred to as Active Galactic Nuclei (AGNs). The AGNs have stronger emission at the compact core which has a much higher luminosity than the rest of the galaxy. A wide range of objects are grouped under the name of AGNs which show some common properties (e.g., high emission power) but usually AGNs show different properties. The currently accepted interpretation is that different properties of AGNs depend on their orientation toward the observer's frame. Roughly 10% of radio loud AGNs (i.e., the radio (5 GHz) to optical (B-band) flux ratio is $>$ 10), have a highly collimated linear structure of plasma– a jet that continuously extracts energy from the central source. This jet happens to play a crucial role in understanding the physical processes in AGNs and their classifications. First, these jets can extend to several hundreds of kiloparsecs into the space often remaining highly collimated, and they are strong sources of radiation in all the accessible bands of the electromagnetic spectrum. Second, depending on the orientation of the jet, the AGN can have different appearances. According to the unification scheme, an AGN is called a blazar when the jet is closely aligned with the line of sight of the observer. Or when the jet's inclination angle is larger, the AGN appears as a radio galaxy.

Blazars are the extreme sub-class of AGNs characterized by high radio and optical polarization, apparent superluminal motion along with high-amplitude variability in all accessible bands of the electromagnetic spectrum. Blazars emission is dominated by non-thermal emission from the jet which is significantly Doppler amplified since the jet with superluminal motion is viewed at small angles. The emission from blazars is observed in a wide frequency range, from radio to high energy (HE; $>$ 100 MeV) and very high energy (VHE; $>$ 100 GeV) γ-ray bands, displaying a double hump structure in their broadband spectral energy distribution (SED). The first component (low-energy) usually peaks between far infrared and X-rays while the second component (HE) is observed between X-rays and HE/VHE γ-rays. The fact that blazars can be observed in almost all energy bands of the electromagnetic spectrum, makes them interesting targets for multiwavelength studies. The single-band observations of blazars give a specific local view of the ongoing complex emission processes, and in order to draw a general picture of the nature of blazar emission, it is necessary to combine the results from the observations in different bands. The combined data from radio to VHE γ-ray bands provide a unique chance to understand their physics.

In the recent years, the accumulation of a significant amount of multiwavelength data and its continuous increase create conditions necessary for further exploration of the physics at work in blazar jets. Namely, it is possible to investigate the multiwavelngth variability of blazars, covering a wide range of timescales; it is necessary for comprehensive study of formation of emission components in blazar SEDs. However, new methods should be adopted to deal with the available large amount of data and its interpretation, i.e., more efficient methods should be used to analyze the data as well as more detailed theoretical modeling is required.

Aim of the thesis

The aim of the thesis is to investigate the optical/UV and X-ray emission properties of a large number of blazars by analyzing the data accumulated in different periods. In particular, the aims are:

- to investigate spectral and temporal properties of X-ray emission from blazars by analyzing the Swift-XRT data of all blazars observed by Swift at least 50 times between December 2004 and the end of 2020;
- to study the emission from blazars in the optical/UV band by analyzing Swift UVOT data accumulated between December 2004 and the end of 2020;
- to investigate the variability of PKS 2155-304 ($z = 0.116$) and S5 0716+71 ($z = 0.31$) emission in the optical/UV, X-ray and γ-ray bands by analyzing data from Fermi-LAT, Swift XRT and Swift UVOT telescopes;
- to study the origin of long-term multiwavelength emission from CTA 102 by performing detailed temporal and spectral analyses of γ-ray, X-ray, and UV/optical data observed by Fermi-LAT, Swift XRT, NuSTAR, and Swift-UVOT;
- to investigate the origin of broadband emission from PKS 0537-286 ($z = 3.1$) using data accumulated during more than ten years from the Fermi-LAT together with Swift UVOT/XRT archival data taken between 2005 and 2017.

Scientific novelty

In this thesis novel methods are used to develop tools which perform complete analysis of the optical/UV and X-ray data observed by Swift XRT. Using these tools, a new multi-temporal easy accessible database of blazars emission in optical/UV and X-ray bands was developed. This unprecedented dataset allows to describe the general temporal and spectral behavior of blazars of different types as well as to compare and contrast the emission properties of 65 blazars which is crucial for understanding the origin of emission from their jets. In the case of different types of blazars (LBL, IBL and HBL), the investigation of (1) their long-term variability and flux variations between the neighboring snapshots, (2) the study of spectral changes correlated with the intensity and (3) the variation of synchrotron peak frequency, contain a valuable information on the physical processes responsible for the X-ray emission. The estimated strong correlation for PKS 2155- 304 emission in the UV and γ-ray bands suggests a common origin of the emission in these bands, i.e., the emission is produced by the same electron population. Similarly, the optical/UV and X-ray emission of S5 0716+71 are correlated, implying a co-spatial origin of the emission. The modeling of 117 contemporaneous SEDs of CTA 102 allowed to systematically study the emission components in the quiescent and flaring periods of the source as well as to estimate the parameters of the emitting electrons (power-law index, cut-off energy, luminosity) and of the jet (magnetic field, Doppler boost factor) and investigate their evolution in time. The multiwavelength studies of distant blazar PKS 0537-286 show that it is a powerful emitter in the X-ray and γ-ray bands; the integrated luminosity of these components exceeds that of the low-energy component (from radio to optical bands).

Practical value

The database for optical/UV and X-ray observations of 65 blazars has a wide application for studying the physics of blazars. In particular, containing comprehensive details on the X-ray and optical/UV emission properties of 65 blazars, this database is unique for studying the variability of blazars as well as for exploring intraband temporal correlations. The results of theoretical modeling are important for investigating the physical conditions of the plasma in different types of blazars. The analysis of correlation between the optical-UV-X-ray and γ-ray emission of PKS 2155-304 and S5 0716+71 allows to probe emission process in their relativistic jets. The modeling of simultaneous SEDs from CTA 102 observations in different periods provides an insight into the dynamical changes of different emission components, which is very useful for understanding the particle acceleration and emission processes.

Basic results to be defended

1. A database of X-ray spectra, best-fit parameter values, count rates and flux estimations in several energy bands of over 31 000 X-ray observations and single snapshots of 65 blazars has been released. By studying the long-term light curves of all sources in the sample, it is shown that a large X-ray luminosity variability on different time-scales is present in all objects. Also, spectral changes are frequently observed with a 'harder-when-brighter' or 'softer-when-brighter' behavior, depending on the SED type of the blazars.
2. A database containing the flux of 65 blazars from more than 13600 Swift UVOT observations in the V, B, U and W1, M2 and W2 bands has been released.
3. It is shown that the multiwavelength emission of PKS 2155-304 ($z = 0.116$) and S5 0716+71 ($z = 0.31$) bright blazars in the optical/UV, X-ray and γ-ray bands is variable, showing multiple flares. In the optical/UV bands, the flux of both sources increased above 2×10^{-10} erg cm^{-2} s^{-1}. The X-ray emission from PKS 2155-304 was characterized by a harder-when-brighter trend, whereas the γ-ray emission from S5 0716+71 showed a moderated trend of softer-when-brighter. The

correlation analysis shows a strong correlation between the UV and γ-ray emission of PKS 2155-304, while there is a correlation between the optical/UV and X-ray emission of S5 0716+71.

4. The long-term multiwavelength emission of CTA 102 ($z = 1.037$) is investigated by performing detailed temporal and spectral analyses of the γ-ray, X-ray and UV/optical data observed by Fermi-LAT, Swift XRT, NuSTAR and Swift-UVOT over a period of 14 years. A strong variability of emission of the source in all the considered bands is found, especially in the γ-ray band it exhibited extreme outbursts when the flux crossed the level of 10^{-5} photon cm^{-2} s^{-1}. In the considered period, 117 high-quality (quasi) contemporaneous SEDs including sufficient multiwavelength data were selected and modeled within a one-zone leptonic synchrotron and inverse Compton emission scenario, assuming that the emitting region is within the broad-line region and considering internal and external seed photons for the inverse Compton up-scattering. The characteristics of the relativistic electrons' distribution in the jet as well as jet properties are retrieved and their variation in time is investigated. The obtained results are discussed in the context of particle cooling in the emitting region.
5. The origin of broadband emission from PKS 0537-286 was investigated by analyzing data accumulated during more than ten years. In the γ-ray band the peak flux of $F_\gamma = (6.23 \pm 0.56) \times 10^{-7}$ photon cm^{-2} s^{-1} was observed on MJD 57874 within one week, which corresponds to $L_\gamma = 2.46 \times 10^{49}$ erg s^{-1} isotropic γ-ray luminosity. It is found that the emission in the X-ray band is characterized by a significantly hard photon index, $\Gamma_{X-ray} \leq 1.3$ and an X-ray flux of 4×10^{-12} erg cm^{-2} s^{-1}, which is almost constant over twelve years. The SED is modeled within one-zone leptonic models, assuming the emission region is within the broad-line region. The modeling shows that the nonthermal electrons in the jet of PKS 0537-286 have a hard power-law index (< 1.9) and that the jet should be particle-dominated with a luminosity within $10^{45} - 10^{46}$ erg s^{-1}.

Approbation of the work

The results of the thesis were presented in Sixteenth Marcel Grossmann Meeting MG16 (Virtual Meeting - July 5-10, 2021) as well as frequently presented and discussed at the seminars of ICRANet Armenia center IO.

Publications

Five papers are published on the topic of the thesis.

Structure of the thesis

The thesis consists of Introduction, four chapters, conclusion and References. The thesis contains 119 pages, including 36 figures and 10 tables.

Content

In **Introduction** the scientific literature related to the topic is reviewed, the novelty of the topic is discussed as well as the aims of the work, the scientific novelty and the main results obtained in each chapter is presented.

In **chapter 1** the main processes of interaction (synchrotron radiation and inverse Compton scattering) of accelerated electrons inside the jet are briefly discussed. Also, the main properties of Fermi Large Area Telescope (Fermi-LAT) and The Neil Gehrels Swift Observatory (Swift) is presented together with main steps to analyse the data obtained by these telescopes.

In **chapter 2** the X-ray emission properties of a large number of blazars are discussed. Namely, it is presented a detailed X-ray spectral, imaging and timing analysis of all the observations and single snapshots of a sample of 65 blazars that have been observed by Swift more than 50 times over a period of 16 years, from launch to the end of 2020. observed many times between launch in November 2004, and the end of 2020. The list includes 65 objects, 24 of which are HBLs, 12 are IBLs and 29 are LBLs.

The data for these sources was reduced and scientific analysis was performed using *Swift_xrtproc* tool which uses the XRT Data Analysis Software (XRTDAS), and the spectral and imaging analysis tools XSPEC and XIMAGE, included in the HEASoft package. *Swift_xrtproc* executes a complete data reduction, from XRT raw data to calibrated data products. The spectral and imaging data taken in PC or WT mode are analysed following standard procedures. The tool automatically downloads the raw data, generates exposure maps and calibrated data products, generates source and background spectral files, makes pile-up correction if needed, performs spectral fitting using the XSPEC package assuming a power-law ($N(E) = k \times E^{-\Gamma}$) and a log-parabola model ($N(E) = k \times E^{-(\alpha+\beta \mathrm{Log}(E))}$), etc. Using Swift_xrtproc we processed a total of 31,068 Swift XRT observations or individual snapshots of the 65 blazars. This led to the generation of 29,050 X-ray spectra, 21,141 photometric flux estimations, and 206 upper limits. The obtained results confirm with large statistics that the log-parabola model generally fits best the X-ray spectral shape of HBL blazars, while LBL sources are usually best fit by a simple power-law. IBL blazars often show more complex spectra, as in these cases the steep end of the synchrotron component merges into the much flatter inverse Compton component in the X-ray band.

The best-fit spectral data and the X-ray fluxes estimated from the imaging analysis have been combined with archival multifrequency data retrieved using the VOU-Blazars software

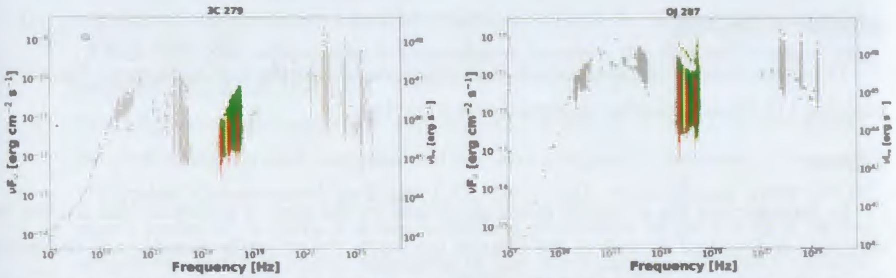

Figure 1: The SEDs of 3C 279 and OJ 287 blazars showing the XSPEC best fit spectra and archival multi-frequency data from VOU-Blazars.

to build the radio to γ-ray SED of each object in the sample. In Figure 1 the SEDs of 3C 279 and OJ 287 are shown. The data from Swift_xrtproc tool are in green, red and light- yellow while grey points are the archival data. The 1 keV flux variation of all the blazars in the sample is also investigated. 1 keV $\nu f(\nu)$ light curves covering the period November 2004 to the end of 2020 of all the sources in the sample can be accessed on-line (https://openuniverse.asi.it/blazars/swift/). Figure 2 show examples of light curves of 3C 273 and Mrk 421. Large luminosity variability on different amplitudes and timescales, ranging from factor of a few to over a factor 200, is present in all sources. The analysis of Swift XRT data of 65 blazars observed at least 50 times shows with large statistics that ν_{peak} in blazars ranges from ~ 10^{12} Hz, to well over 10^{18} Hz, the position of ν_{peak} is not constant in time. Our results show that frequent and large variations of ν_{peak}, spanning a range of well over a factor 100 in some objects, is a very common, likely ubiquitous, feature of HBLs. Most of the X-ray flux enhancements in HBL sources is due to the effects of spectral hardening, rather than to an overall flux increases at all energies.

In the **chapter 3** the variability of blazars in the optical band is investigated. The emission from jets of blazar ranges across all accessible bands in the electromagnetic spectrum so their multi-wavelength observations are essential for the study of the origin of their emission. Sometimes (but not always) there is a correlated variability between two bands which indicates that the same process might be responsible for the emission in these bands. Now, the accumulated amount of data permits a detailed variability study in almost all the bands which is crucial for understanding the complex physics of blazars. The multiwavelength variability study of blazars has recently entered a new era. There is a large amount of γ-ray data available from continuous observations of blazars in the HE band by Fermi-LAT. Also, Swift performed a large number of observations of single objects. For this purpose, a tool that automatically downloads and analyses data from Swift UVOT observations of blazars was developed. The Swift UVOT telescope can produce images in each of six filters, namely in V (500-600 nm), B (380-500 nm), U (300-400 nm), W1 (220-400 nm), M2 (200-280 nm) and W2 (180-260 nm). Providing the name and the coordinates of the source under interest, it

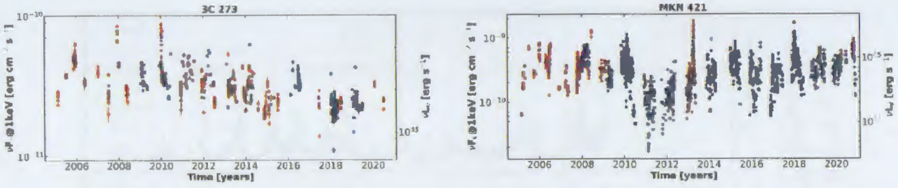

Figure 2: The 1 keV light curves of 3C 273 and Mrk 421 blazars.

accesses the Swift archive, downloads all the existing observations and processes them with the standard procedure. After cleaning and filtering the data, all single observations are reduced by selecting source counts from a circular region of 5" around the source, while selecting the background counts from a 20" region away from the source. Then with the help of uvotsource tool it derives the magnitudes which are converted to fluxes using the conversion factors and then corrected for extinction, using the reddening coefficient $E(B-V)$ from the Infrared Science Archive (http://irsa.ipac.caltech.edu/applications/DUST/). The tool produces the flux measured in each filter in each period for the light curve computation as well as the flux for each frequency for SED calculations. The tool was used to analyze all the Swift UVOT observations available from observations of blazar (the results are available here https://github.com/DavidIsrayelyan/Swift-UVOT-Database).

The developed tool was used to analyse all the Swift UVOT observations of PKS 2155-304 and S5 0716+71. Between 2004 - 2022, PKS 2155-304 was observed 300 times and S5 0716+71 - 352 times. The light curve of PKS 2155-304 shows that during the initial observations (e.g., until MJD 55000) the source was in an evaluated emission state in all the considered bands. For example, in this period the highest flux of the source was $(3.12 \pm 0.07) \times 10^{-10}$ erg cm^{-2} s^{-1} observed on MJD 53960.85 in filter M2. Then the averaged level of source emission in optical/UV bands decreases, but a few times flux variations in all the considered filters are still evident. For example, the flux in M2 band on MJD 56046.13 was $(5.1 \pm 0.11) \times 10^{-11}$ erg cm^{-2} s^{-1} which increased to $(1.60 \pm 0.03) \times 10^{-10}$ erg cm^{-2} s^{-1} on MJD 56180.67. Such changes in consecutive UVOT observations can be identified during all the considered periods, which show that this source has a strongly variable optical/UV emission.

In the light curve of S5 0716+71 two large flaring activities in optical and UV bands are evident. The first active period was observed between MJD 57030-57060 when the flux in almost all filters increased from $\sim 5 \times 10^{-11}$ erg cm^{-2} s^{-1} to above $\sim 2 \times 10^{-10}$ erg cm^{-2} s^{-1}. In this period, the highest flux of $(3.28 \pm 0.09) \times 10^{-10}$ erg cm^{-2} s^{-1} was observed in filter V on MJD 57047.31. The next major flaring activity was observed between MJD 58200-58300 when the flux again increased above ~ 2×10^{-10} erg cm^{-2} s^{-1}. This source is characterized by variable optical/UV emission, i.e., the flux changes in different Swift observations. Only between MJD 56600-56800 the source was in a relatively quiescent

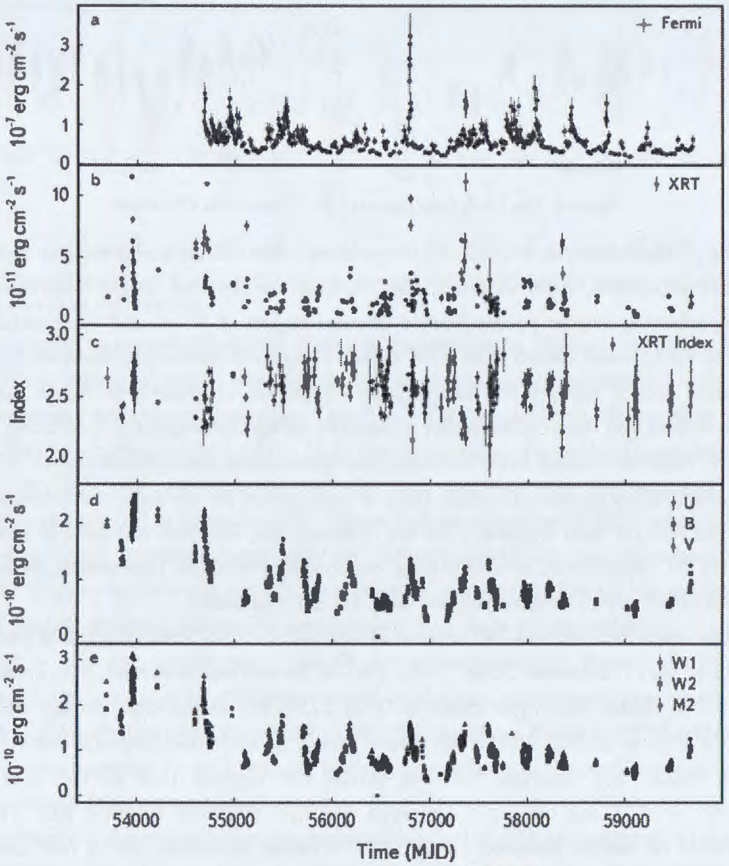

Figure 3: Multiwavelength light curve of PKS 2155-304.

state in the optical/UV bands: during this period, in 14 *Swift* observations the flux was relatively constant with a value of ~ 2×10^{-11} erg cm^{-2} s^{-1}.

The multiwavelength light curves of PKS 2155-304 and S5 0716+71 show contemporaneous changes in the flux in different bands. In order to test whether or not the emission in different bands is varying contemporaneously, i.e., whether the emission in different bands is related, a Spearman correlation test was applied. The possible correlation was investigated by computing the correlation rank between the emission in different bands, i.e., computing Spearman correlation coefficient ρ. In order to perform an as general as possible test, the correlation between the emission in the X-ray and γ-ray bands, X-ray and optical/UV bands, γ-ray and optical/UV bands was investigated. The results from the Spearman correlation analysis are given in Table 1 for each two bands providing the coefficient and probability. The results reported in Table 1 show that the null hypothesis that there is no correlation can be rejected in all cases. However, there is no strong correlation between the emissions in different bands. For PKS 2155-304, the strongest correlation is found for UV and γ-ray bands, $\rho = 0.8$ (Figure 4 left). There is also a milder correlation between the source emission in X-ray and optical bands with $\rho = 0.6$. For S5 0716+71, there is again a weak correlation between the emission in the X-ray and γ-ray bands with $\rho = 0.5$ (Figure 4 right). For this source, the correlation is almost at the same level for the optical/UV vs X-ray and optical/UV vs γ-ray bands (see Table 1)).

		PKS 2155-304		S5 0716+71	
Band-1	Band-2	Spearman coeff.	p-value	Spearman coeff.	p-value
Optical	X-ray	0.6	1.3e-22	0.7	3e-44
UV	X-ray	0.6	3.5e-30	0.7	1.3e-46
Optical	γ -ray	0.7	5.4e-18	0.6	4.8e-18
UV	γ -ray	0.8	3.6e-19	0.7	1.3e-18
X-ray	γ -ray	0.5	6.1e-8	0.5	2.4e-12

Table 1: Results of the correlation study between the emission in different bands.

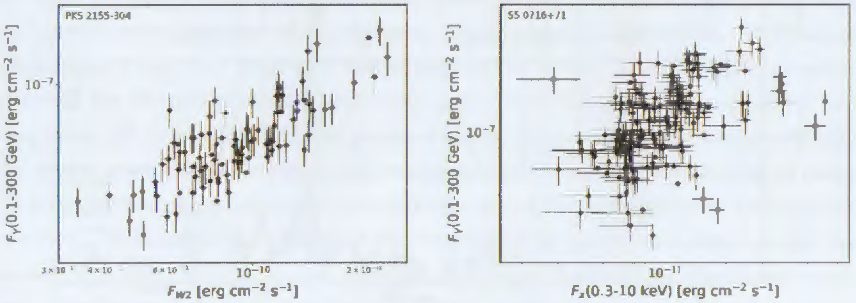

Figure 4: The scatter plot of the flux in different bands.

In the **chapter 4** the multiwavelength emission from the CTA 102 was investigated. CTA 102 is a FSRQ with a redshift of $z = 1.037$. Harboring a black hole with a mass of $8.5 \times 10^{8}\ \mathrm{M}_{\odot}$, CTA 102 is one of the brightest FSRQs observed in the HE γ-ray band. It was initially observed by the Compton Gamma Ray Observatory mission having estimated a γ-ray flux of $(2.4 \pm 0.5) \times 10^{-7}$ photon cm^{-2} s^{-1}. Then, CTA 102 was scanned continuously by Fermi-LAT since mid-2008, initially showing that the source is relatively weak in the γ-ray band. However, from 2016 to 2017 it underwent an unprecedented outburst in all the wavebands. Motivated by the availability of multiwavelength data from CTA 102 observations before, during and after the large outburst, for furthering our knowledge of the emission processes dominating in the jet of CTA 102 we performed an intense broadband study of CTA 102 by analyzing data accumulated by Fermi-LAT, Swift XRT, Nustar, Swift UVOT accumulated during 2008-2022. We have systematically investigated the spectral and variability properties of the source emission in the optical/UV, X-ray and γ-ray bands. The

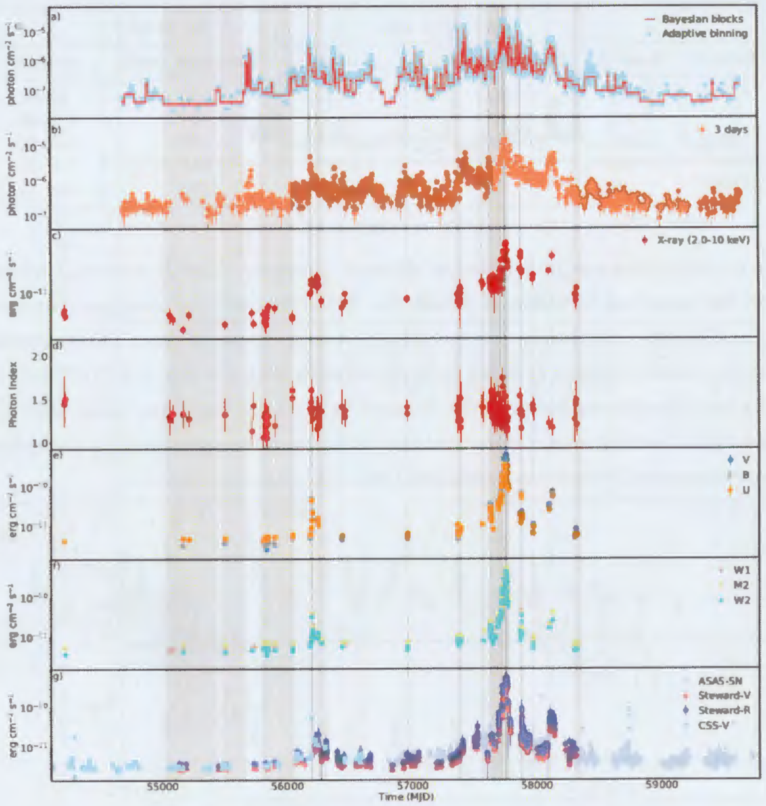

Figure 5: The multiwavelength light curve of CTA 102.

multiwavelength light curve of CTA 102 in the γ-ray (Fermi LAT), X-ray (Swift XRT) and optical bands (Swift UVOT, ASAS-SN and Catalina Sky Survey) are shown in Figure 6. In all the considered bands, the source shows multiple periods with significant brightening. For example, in the γ-ray band the highest flux of $(2.64 \pm 0.6) \times 10^{-5}$ photon cm^{-2} s^{-1} above 166.3 MeV was observed on MJD 57738.5 or in the X-ray band the highest flux was $F_{X-ray}[2-10\,kev] = (5.77 \pm 0.63) \times 10^{-11}$ erg cm^{-2} s^{-1}. The analyzed data were used to follow the evolution of the emission spectrum in different bands. The evolution of the CTA 102 SEDs in time is shown here (https://youtu.be/jFNkI_psAjo). These SEDs were generated by plotting the γ-ray spectra for each of the Bayesian blocks shown in Figure 6 together with the data available in all other energy bands. This animation shows the high-amplitude and spectral changes in different periods, demonstrating dramatic changes of the CTA 102 during the prolonged outbursting period.

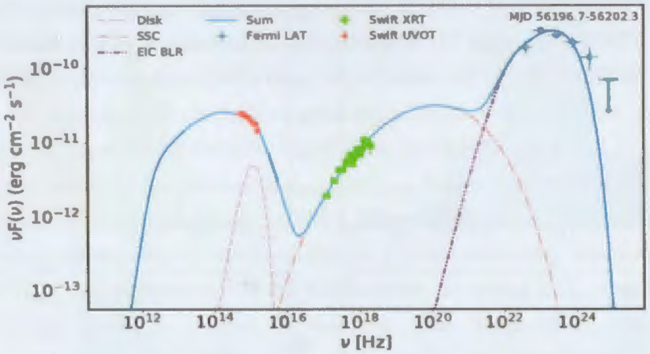

Figure 6: The multiwavelength SED of CTA 102 during MJD 56196.7-56202.3.

In order to model the SEDs of CTA 102 in different periods, from the SEDs generated for each Bayesian block there were selected all the periods with sufficient multiwavelength data, i.e., when the optical/UV data at least in two filters is available together with the γ-ray and X-ray data. In Figure 6 the selected periods are shown in gray. As a result, high-quality SEDs in 117 periods were assembled which represent various emitting sates of CTA 102 including periods when it was in a prolonged flaring state in the γ-rays. Therefore, this allows to understand the physical processes dominating in the jet of the source in its quiescent and flaring states. All the selected SEDs are modeled within the same one-zone scenario. Within this scenario, the accelerated electrons (protons) are injected in the spherical region of radius R. This magnetized region with a field strength of B moves along the jet with a bulk Lorentz factor of Γ_{jet} at an angle of θ relative to the observer's line of sight. It is assumed that the spectrum of the injected electrons is described by a power-law with an exponential cutoff energy distribution defined as $N(\gamma_e) = N_0 \gamma_e^{-p} \mathrm{Exp}\,(-\gamma_e/\gamma_{cut})$, $\gamma_e > \gamma_{min}$. In this scenario, the first peak in the SED is described by synchrotron radiation as a consequence of the interaction of relativistic electrons inside the emitting region with the magnetic field. Instead, the second peak (from X-ray to HE γ-rays) is formed by the contribution of inverse Compton scattering of synchrotron (SSC) and BLR reflected (EIC) photons. The BLR radius and luminosity of CTA 102 are $R_{BLR} = 6.73 \times 10^{17}$ cm and $L_{BLR} = 4.14 \times 10^{45}$ erg s^{-1}, respectively, and the BLR is modelled as a spherical shell with a lower boundary of $R_{in,BLR} = 0.9 \times R_{BLR} = 6.06 \times 10^{17}$ cm and an outer boundary of $R_{out,BLR} = 1.2 \times R_{BLR} = 8.08 \times 10^{17}$ cm. Assuming that the 10% of the disc luminosity is reprocessed into BLR radiation, the disc luminosity would be $L_{disc} = 4.14 \times 10^{46}$ erg s^{-1}.

To model the broadband SED, a publicly available code, JetSet was used. The multiwavelength SED of CTA 102 constrained with contemporaneous data observed during MJD 56196.7-56202.3 and modelled with JetSet is shown in Figure 5. The dashed violet line shows the disc thermal emission approximated as a black body. The power-law index of the emitting electrons is p = 1.61 while the minimum and cut-off energies are $\gamma_{min} = 51.3$ and

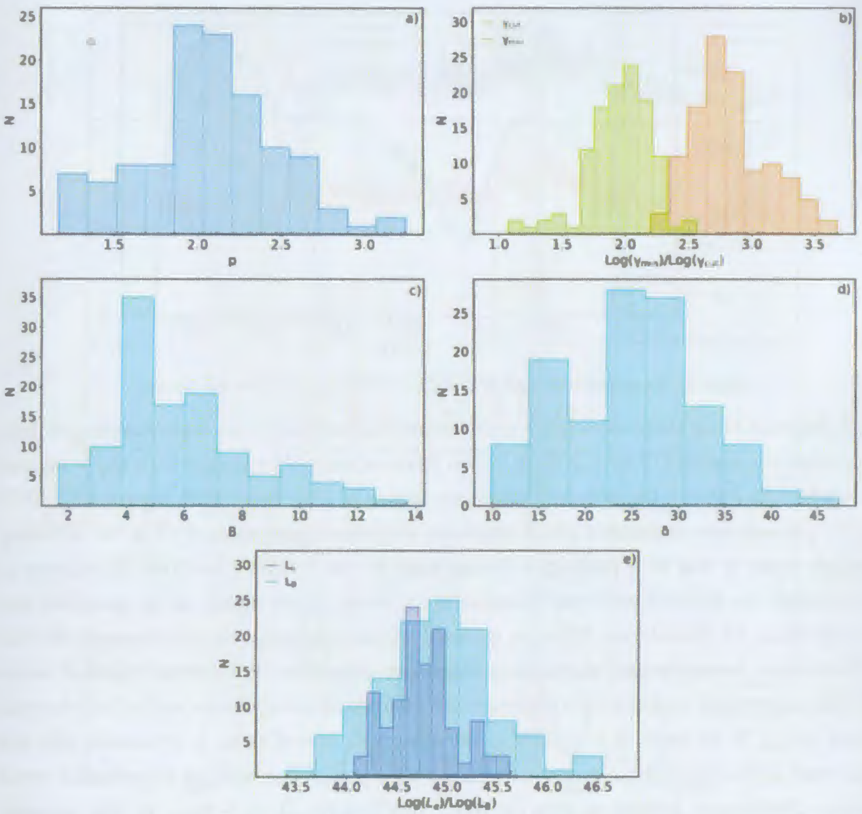

Figure 7: The distribution of the parameters obtained from the fitting of all data-sets composed with simultaneous data.

$\gamma_{cut} = 685.6$, respectively. The synchrotron emission of these electrons in the magnetic field of B = 4.43 G extends up to 10^{16} Hz explaining the observed data in the optical/UV bands. Then, the SSC component takes into account the X-ray data (orange dashed curve in Figure 5) dominating only up to 10^{22} Hz, failing to explain the γ-ray data. Instead, the inverse Compton upscattering of the BLR photons that have higher mean energy and number density in the jet frame can explain the γ-ray data (purple dot-dashed curve in Figure 5). The modelling allows to estimate the jet parameters such as size of the emission region, R = 2.03×10^{15} cm and the Doppler factor $\delta = 29.8$. The size of the emission region corresponds to the flux variability of the order of 1.3 hours, consistent with the rapid multi-band variability of CTA 102.

The modelling of the single snapshot SED shown in Figure 6 permits to identify the parameters of the emitting region and the jet for a given period. However, in order to deeply investigate the multiwavelength emission processes in CTA 102 something beyond the single-epoch SED modelling is required. The modeling of 117 high-quality SEDs of CTA 102 observed in different periods is available here https://youtu.be/ 0H1IyNN9PSM. This allows to investigate the properties of the jet and emitting particles over time. For example, the power-law index of the emitting electron distribution varies between $p = 1.17 - 3.25$ with a mean of $p_{\rm mean} = 2.08$, the distribution of $\gamma_{\rm min}$ and $\gamma_{\rm cut}$ have a narrow distribution peaking around $\gamma_{\rm min,mean} = 104.6$ and $\gamma_{\rm cut,mean} = 905.1$, respectively, etc.

The modelling allows also to estimate the jet power carried by electrons (L_e) and magnetic field (L_B). The distribution of the luminosities computed as $L_e = \pi c R_b^2 \Gamma^2 U_e$ and $L_B = \pi c R_b^2 \Gamma^2 U_B$ is shown in Figure 7 panel e). The mean of L_e and L_B is at 7.81×10^{44} erg s^{-1} and 2.07×10^{45} erg s^{-1}, respectively. The distribution of L_B in the range $2.51 \times 10^{43} - 3.48 \times 10^{46}$ erg s^{-1} is broader than that of L_e between $1.20 \times 10^{44} - 4.21 \times 10^{45}$ erg s^{-1} . The large variations of L_B are mostly due to the high-amplitude changes of the synchrotron component in the SED of CTA 102. Instead, the high-amplitude increase of the γ-ray flux interpreted as EIC of BLR photons which would affect the electron content in the jet is compensated by increasing δ. The distribution of L_e and L_B in Figure 7 panel e) shows that in some periods $L_e/L_B < 1$, i.e., the jet is magnetically dominated. Such a trend is observed when the synchrotron component (defined by optical/UV data) exceeds the SSC component (defined by X-ray data).

The estimated parameters allow also to assess the total kinetic energy of the jet, namely, assuming a proton-to-electron comoving number density ratio of $N_p/N_e \simeq 0.1$, the total kinetic luminosity defined as $L_{kin} = L_e + L_B + L_{p,cold}$ varies from 4.64×10^{44} erg s^{-1} to 3.71×10^{46} erg s^{-1}. The central black hole mass in CTA 102 is estimated to be 8.5×10^{8} $M_{\rm BH}$, so the Eddington luminosity is $\simeq 1.1 \times 10^{47}$ erg s^{-1}. Therefore, the kinetic power of the jet estimated in various periods is lower than the Eddington luminosity.

In the **chapter 5** the origin of multiwavelength emission from PKS0537-286 is investigated. PKS 0537-286, at $z = 3.104$, is a luminous blazar included in the fourth catalog of AGNs detected by Fermi-LAT. It has been frequently observed in the X-ray band with various instruments which showed that it is a very bright source with a luminosity of $L_{x-ray} = 10^{47}$ erg s^{-1} between 0.1 - 1 keV. Considering multiple observations of PKS 0537-286 with the Swift observatory carried out between 2005 and 2017 which provide data in both optical/UV and X-ray bands as well as more than ten years of data in the γ-ray band accumulated by Fermi-LAT, PKS 0537-286 has become an ideal object for exploring the physics of blazars. Swift observed PKS 0537-286 16 times between 2005 and 2017. All UVOT and XRT data, expect ObsID 00030816011 with an extremely short exposure (159.4 sec), were extracted and analyzed. The results are given in Table 2, where for each observation, the ObsID, date, exposure, photon index Γ, flux and C-stat/d.o.f. are provided. The X-ray flux

Obs. ID	Date	Exp. Time (s)	Γ^a	Flux^b	C (d.o.f.)
30816001	Oct 27, 2006	3040	1.09 ± 0.17	4.18 ± 0.74	1.07 (156)
30816003	Oct 30, 2006	3894	1.33 ± 0.13	4.09 ± 0.55	1.12 (197)
30816004	Oct 31, 2006	4425	1.27 ± 0.14	3.62 ± 0.50	0.97 (201)
30816005	Feb 10, 2008	6708	1.10 ± 0.11	4.58 ± 0.42	1.23 (278)
30816006	Feb 12, 2008	5274	1.01 ± 0.13	4.14 ± 0.57	1.11 (226)
30816007	Feb 14, 2008	4822	1.11 ± 0.13	4.16 ± 0.57	1.14 (215)
30816008	Oct 07, 2008	1593	1.04 ± 0.29	3.29 ± 0.98	0.68 (65)
30816009	Mar 12, 2010	1076	1.00 ± 0.34	3.82 ± 1.34	0.91(51)
30816010	Mar 12, 2010	2018	0.93 ± 0.32	2.07 ± 0.69	1.28(49)
30816012	Sep 06, 2011	3931	1.06 ± 0.18	3.01 ± 0.57	0.86(135)
35240001	Nov 23, 2005	9038	1.17 ± 0.10	3.51 ± 0.37	0.87(306)
35240002	Dec 8, 2005	14750	1.13 ± 0.08	3.84 ± 0.40	1.08(407)
36783001	May 17, 2007	5414	1.32 ± 0.11	4.20 ± 0.48	1.12(257)
36783002	May 10, 2017	1933	1.28 ± 0.20	4.28 ± 0.87	1.09(116)
36783003	May 12, 2017	2238	1.03 ± 0.19	4.52 ± 0.91	0.98(123)
Swift UVOT					
	U	W1	M2	B	V
30816008	20.8 ± 1.2	21.5 ± 1.8	21.9 ± 4.4	19.7 ± 0.4	19.3 ± 0.6
30816009	21.0 ± 1.0	20.2 ± 0.5	21.0 ± 0.9	20.0 ± 0.3	18.7 ± 0.3
35240002	20.8 ± 0.1	22.0 ± 2.1	21.3 ± 1.1	19.5 ± 0.3	18.8 ± 0.3

Table 2: Fitting results of the data obtained by the XRT instrument on board SWIFT.

(0.3-10 keV) varies in the narrow range of $F = (3.01 - 4.58) \times 10^{-12}$ erg cm^{-2} s^{-1} being almost constant during the twelve years of observation of PKS 0537-286. Interestingly, the X-ray emission is characterized by a substantially hard photon index of < 1.3 which implies that in νF_ν representation the X-ray spectrum has an increasing shape. Considering only the observations with counts > 100, which allow confidential estimation of the parameters, the hardest photon index is 1.03 ± 0.19 observed on May 12, 2017. For most of the Swift UVOT observations, in several filters, the counts were not enough to measure the source magnitude and only for ObsIDs 00030816008, 00030816009 and 0003524002 five filters were available.

The γ-ray flux and photon evolution in time were investigated by generating the light curves using the unbinned likelihood analysis method implemented in the gtlike tool. The flux and photon index were measured in each time interval, restricting the energy range to (0.1-300) GeV and assuming a power-law spectrum for PKS 0537-286. The γ-ray flux in time, the light curve is generated with a month time binning (Figure 8). There is a clear indication of flux variability with several times when the flux was above 10^{-7} photon cm^{-2} s^{-1}. One

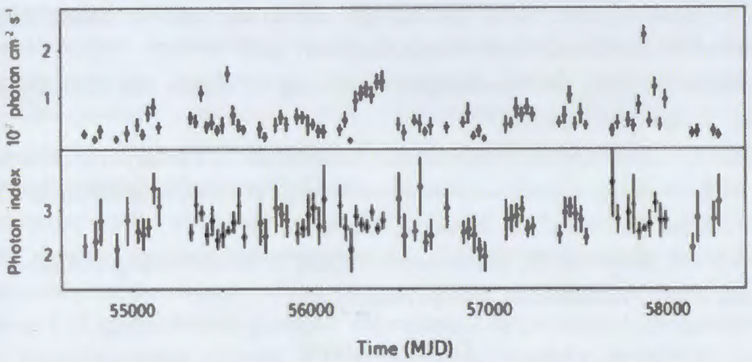

Figure 8: The γ-ray light curve and the photon index of PKS 0537-286.

of such periods starts from MJD 56272 and lasts for 30 days. The highest flux corresponds to $(2.32 \pm 0.19) \cdot 10^{-7}$photon cm^{-2} s^{-1} observed during the major flare mentioned above.

The SED of PKS 0537-286 was modeled with one-zone scenario and the results are shown in Figure 9. Initially, the SED is modelled assuming that only synchrotron photons are inverse Compton up-scattered to higher energies, neglecting the external photons (solid line in Figure 9 left panel). The modeling shows that the emitting electrons are distributed with an index of $\alpha = 1.48$, the cut-off energy of electrons is $\gamma_{cut} = 5138.4$, the minimum energy of the electrons was estimated to be at $\gamma_{\min} = 7.34$, and the magnetic field $B = 44.8$ mG. The results of the SED modelling when both internal and external photons are considered (SSC+EIC) is shown Figure 9 (right panel). In this case the same parameters are: $\alpha = 1.95$, $\gamma_{cut} = 694.6$ and $B = 0.81$ G.

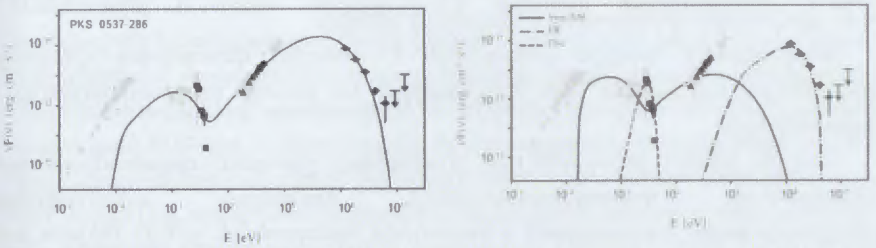

Figure 9: The broadband SED of PKS 0537-286. *Left panel:* The modeling considering only the SSC model. *Right panel:* The modeling considering both synchrotron (SSC) and external photons (EIC).

Publications in the topic of thesis

1. Giommi P., Perri M., Capalbi M., D'Elia V., Barres de Almeida U., Brandt C., Pollock A., Arneodo F., Di Giovanni A., Chang Y., Civitarese O., De Angelis M., Leto C., Verrecchia F., Ricard N., Di Pippo S., Middei R., Penacchioni A., Ruffini R., Sahakyan N., **Israyelyan**

D., Turriziani S., 2021, *X-ray spectra, light curves and SEDs of blazars frequently observed by Swift*, Mon. Not. R. Astron. Soc., 507, 5690.

2. **Israyelyan D.**, 2022, *Multiwavelength Monitoring Of Blazars Pks 2155-304 And S5 0716+71*, Astrophysics, 65, 315.
3. Sahakyan N., **Israyelyan D.**, Harutyunyan G., Gasparyan S., Vardanyan V., Khachatryan M., 2022, *Modeling the time variable spectral energy distribution of the blazar CTA 102 from 2008 to 2022*, Mon. Not. R. Astron. Soc., stac2875.
4. Sahakyan N., **Israyelyan D.**, Harutyunyan G., 2020, *A Multiwavelength Study of Distant Blazar PKS 0537-286*, Astrophysics, 63, 459.

ԱՄՓՈՓԱԳԻՐ

Բլազարներն ակտիվ գալակտիկական միջուկների ենթադաս են, որոնց շիթն ուղղված է դեպի դիտողը, և Դոպլեր ուժեղացման շնորհիվ՝ ճառագայթումն ավելի պայծառ է դիտողի համար։ Բլազարները տիեզերքի էլեկտրամագնիսական ճառագայթման ամենապայծառ, կայուն աղբյուրներն են, որոնց ճառագայթումը միշտ ուսումնասիրվում է տարբեր ալիքային տիրույթներում գործող դիտակներով։ Բազմաալիքային տիրույթում գրանցված տվյալները թույլ են տալիս իրականացնել մանրամասն սպեկտրալ և ժամանակային վերլուծություն, ինչը կարևոր է բլազարների շիթերում մասնիկների ճառագայթման մեխանիզմներն ուսումնասիրելու համար։ Ատենախոսությունում ուսումնասիրվել է բլազարների օպտիկական/գերմանուշակագույն և ռենտգենյան տիրույթներում ճառագայթման հատկությունները, ինչպես նաև բլազարների բազմաալիքային տիրույթում ճառագայթման մեխանիզմներն։ Ատենախոսությունը կազմված է ներածությունից, հինգ գլուխներից, վերջաբանից և հղումների ցանկից։

Առաջաբանում հակիրճ քննարկված է թեմային վերաբերվող գիտական գրականությունն, ինչպես նաև ներկայացված են թեմայի արդիականությունը և նպատակները։

Առաջին գլխում քննարկվել են բլազարների շիթերում ռելյատիվիստական էլեկտրոնների փոխազդեցությունների հիմնական մեխանիզմները (սինքրոտրոնային ճառագայթում և հակադարձ Կոմպտոնյան ցրում)։ Ինչպես նաև ներկայացվել է Swift XRT/UVOT և Fermi-LAT դիտակների հիմնական բնութագրերը և դրանցով գրանցված տվյալների մշակման հիմնական քայլերը։

Երկրորդ գլխում օգտագործելով swift_xrtproc գործիքն՝ իրականացվել է Swift XRT ռենտգենյան դիտակով 2004թ. դեկտեմբերից մինչև 2020թ. վերջ, 50 անգամից ավել դիտված բոլոր բլազարների տվյալների սպեկտրալ և ժամանակային վերլուծություն։ Տվյալների մշակման արդյունքում ստեղծվել է տվյալների բազա, որը ներառում է 65 բլազարների ավելի քան 31000 ռենտգենյան տիրույթի դիտումների սպեկտրերը, ճառագայթման սպեկտրերը նկարագրող լավագույն պարամետրերը և ճառագայթման հոսքը՝ մի քանի էներգիական տիրույթներում։ Հետազոտվել է առանձնացված աղբյուրների հոսքի փոփոխականությունը 1 կէՎ տիրույթում, տարբեր դասերի բլազարների ճառագայթման հոսքի և ֆոտոնային ցուցիչի կախվածությունն, ինչպես նաև աղբյուրների էներգիայի սպեկտրալ բաշխվածությունները (ԷՍԲ)՝ համադրելով վերլուծված տվյալները բազմաալիքային տիրույթի արխիվային տվյալների հետ։

Երրորդ գլխում հետազոտվել են PKS 2155-304 ($z = 0.116$) and S5 0716+71 ($z = 0.31$) պայծառ բլազարների օպտիկական, գերմանուշակագույն, ռենտգենյան և γ տիրույթներում ճառագայթման հատկությունները՝ մշակելով Swift UVOT, Swift XRT և Fermi-LAT դիտակներով գրանցած տվյալները։ Ներկայացվել է ծրագրային փաթեթ, որն իրականացնում է Swift UVOT դիտակով տարբեր տարիների գրանցված տվյալների ավտոմատացված վերլուծություն։ Առանձնացված աղբյուրների համար պատրաստվել են բազմաալիքային տիրույթում լուսային կորերը և հետազոտվել են տարբեր ալիքային տիրույթներում ճառագայթման հոսքերի կոռելյացիաները։ Ցույց է տրվել, որ PKS 2155-304 և S5 0716+71 բլազարների ԷՍԲ-ները, փոփոխականությունները և տարբեր տիրույթներում ճառագայթումների միջև կոռելյացիաները կարող են բացատրվել մեկ տիրույթում գտնվող էլեկտրոնների սինքրոտոնային և սինքրոտոնային ֆոտոնների հակադարձ Կոմպտոնյան ցրման (ՀԿՑ) մոդելների շրջանակում։

Չորրորդ գլխում ուսումնասիրվել է CTA 102 ($z = 1.037$) բլազարի բազմահաճախային տիրույթում ճառագայթման մեխանիզմները՝ վերլուծելով 2008-2022թթ. Swift-UVOT, Swift XRT, NuSTAR և Fermi-LAT դիտակներով օպտիկական, գերմանուշակագույն, ռենտգենյան և γ տիրույթներում գրանցված տվյալները։ Հետազոտվել է նշված տիրույթներում աղբյուրի ճառագայթման հոսքերի կոռելյացիան և ճառագայթման հոսքի փոփոխականությունը, ցույց է տրվել, որ բոլոր տիրույթներում աղբյուրի ճառագայթման հոսքը զգալի աճում է։ Օգտագործելով վերլուծված տվյալները՝ պատրաստվել են աղբյուրի ճառագայթման միաժամանակյա տվյալներով ԷՍԲ-ներ, և հետազոտվել են ճառագայթման տարբեր բաղադրիչների փոփոխությունները ժամանակի ընթացքում (https://youtu.be/jFNkI_psAjo)։ Ստացված ԷՍԲ-երից 117-ը, որոնք ունեն բավարար քանակությամբ տվյալներ, մոդելավորվել են մեկ տիրույթից լեպտոնային մոդելի շրջանակում՝ ենթադրելով, որ ճառագայթման տիրույթը գտնվում է լայն գծերով տիրույթի ներսում և հակադարձ Կոմպտոնյան ցրման համար հաշվի են առնվել, թե՛ ներքին, թե՛ արտաքին ֆոտոնային դաշտերը։ Մոդելավորման արդյունքում գնահատվել են շիթը և ճառագայթող մասնիկները նկարագրող հիմնական պարամետրերը, հետազոտվել դրանց փոփոխությունը ժամանակի ընթացքում։

Հինգերորդ գլխում մանրամասն ուսումնասիրվել է PKS 0537-286 ($z = 3.1$) բլազարի բազմահաճախային տիրույթում ճառագայթման մեխանիզմները, վերլուծելով Swift UVOT/XRT և Fermi-LAT դիտակներով տարբեր տարիների ընթացքում գրանցված տվյալները: Հետազոտվել է աղբյուրի ճառագայթման հոսքի փոփոխականությունը, գնահատվել հոսքը ակտիվ վիճակներում: Ստացված արդյունքները մոդելավորվել են մեկ տիրույթից լեպտոնային մոդելի շրջանակում՝ ենթադրելով, որ ռենտգենյան և γ տիրույթների տվյալներն առաջանում են (i) միայն սինքրոտրոնային ֆոտոնների և (ii) սինքրոտրոնային և արտաքին ֆոտոնների հակադարձ Կոմպտոնյան ցրումից: Մոդելավորման արդյունքները ցույց են տալիս, որ ճառագայթող էլեկտրոնների ֆոտոնային ցուցիչը < 1.9, իսկ շիթում գերակշռում են մասնիկները, որոնց լուսատվությունը $(10^{45} - 10^{46})$ էրգ վրկ$^{-1}$ տիրույթում է:

Резюме

Блазары это подкласс активных галактических ядер, струя которых направлена на наблюдателя, а их излучение для наблюдателя, из-за доплеровского усиления, становится ярче. Блазары самые яркие и стабильные источники электромагнитного излучения во Вселенной, и их излучение всегда изучается телескопами, работающими в разных волновых диапазонах. Данные, зарегистрированные в многоволновом диапазоне, позволяют проводить детальный спектральный и временной анализ, что важно для исследования механизмов излучения частиц в струях блазаров. В диссертации исследованы свойства излучения блазаров в оптическом/ультрафиолетовом и рентгеновском диапазонах, также механизмы излучения блазаров в многоволновом диапазоне. Диссертация состоит из ведения, пяти глав, заключения и списка литературы.

Во введении кратко рассмотрена научная литература по теме, также представлены актуальность и цели темы.

В главе 1 обсуждались основные механизмы взаимодействия релятивистских электронов в струях блазаров (синхротронное излучение и обратное комптоновское рассеяние). Также были представлены основные характеристики телескопов Swift XRT/UVOT и Fermi-LAT, и основные этапы анализа их данных.

В главе 2 с помощью инструмента swift_xrtproc был проведен спектральный и временной анализ данных всех блазаров, наблюдавшихся более 50 раз с декабря 2004 г. по конец 2020 г. с помощью рентгеновского телескопа Swift XRT. В результате обработки данных создана база данных, включающая более 31000 спектров рентгеновских наблюдений 65 блазаров, наилучшие параметры описывающие спектры излучения и потока излучения в нескольких диапазонах энергий. Исследованы переменность потоков источников в диапазоне 1 кэВ, зависимость потока излучения и фотонного индекса различных классов блазаров, а также путем объединения проанализированных данных с архивными данными спектральные распределения энергии (СРЭ) источников.

В главе 3 исследуются излучения ярких блазаров PKS 2155-304 ($z = 0{,}116$) и S5 0716+71 ($z = 0{,}31$) в оптическом/УФ, рентгеновском и γ диапазонах путем анализа данных телескопов Swift UVOT, Swift XRT и Fermi-LAT. Представлено программное обеспечение, выполняющее автоматизированный анализ данных, зарегистрированных данных телескопом Swift UVOT за разные годы. Для каждого источника были построены многоволновые кривые блеска и исследованы корреляции потоков излучения в разных диапазонах волн. Показано, что СРЭ, переменность и корреляция между излучениями в разных полосах блазаров PKS 2155-304 и S5 0716+71 могут быть объяснены в рамках моделей однозонного синхротронного излучения и обратного комптоновского рассеяния синхротронных фотонов.

В главе 4 изучались механизмы излучения блазара CTA 102 ($z = 1{,}037$) в многочастотном диапазоне, путем анализа данных, зарегистрированных в оптическом, ультрафиолетовом, рентгеновском и γ диапазонах с телескопами Swift-UVOT, Swift XRT, NuSTAR и Fermi-LAT в период с 2008 по 2022 годы. Исследована корреляция потоков излучения источника и изменчивости потока излучения в указанных диапазонах, показано, что поток излучения источника значительно увеличивается во всех диапазонах. Используя проанализированные данные, были подготовлены СРЭ излучении источника с одновременными данными и исследовано изменение различных компонентов излучения во времени (https://youtu.be/jFNkI_psAjo). Из подготовленных СРЭ 117, с достаточным объемом данных, были смоделированы в рамках однозонной лептонной модели, в предположении, что источник излучения находится внутри области широких линий, и с учетом как внутренних, так и внешних фотонных полей для обратного комптоновского рассеяния. В результате моделирования были оценены основные параметры, описывающие струю и излучающие частицы, исследовано их изменение во времени.

В главе 5 детально изучены механизмы излучения в многочастотном диапазоне блазара PKS 0537-286 ($z = 3.1$), анализируя данные, зарегистрированные телескопами Swift UVOT/XRT и Fermi-LAT в разные годы. Исследована изменчивость потока излучения источника, оценен поток в активных состояниях. Полученные результаты были моделированы в рамках однозонной лептонной модели, предполагая, что данные в рентгеновском и γ диапазонах возникают за счет (i) только синхротронных фотонов и (ii) обратного комптоновского рассеяния как синхротронных, так и внешних фотонов. Результаты моделирования показывают, что фотонный индекс излучающих электронов < 1.9, а в струе преобладают частицы, светимость которых находится в диапазоне $(10^{45} - 10^{46})$ эрг сек$^{-1}$.

Davit Israyelyan / Դավիթ Իսրայելյան / Давид Исраелян